Host factors in nidovirus replication
Wilde, A.H. de

Cover Page

Universiteit Leiden

The handle http://hdl.handle.net/1887/22212 holds various files of this Leiden University dissertation.

Author: Wilde, Adriaan Hugo de
Title: Host factors in nidovirus replication
Issue Date: 2013-11-13

Chapter 3

Cyclophilin inhibitors block arterivirus replication by interfering with viral RNA synthesis

Adriaan H. de Wilde, Yanhua Li, Yvonne van der Meer, Grégoire Vuagniaux, Robert Lysek, Ying Fang, Eric J. Snijder, and Martijn J. van Hemert

ABSTRACT

Virus replication strongly depends on cellular factors, in particular on host proteins. Here we report that the replication of the arteriviruses equine arteritis virus (EAV) and porcine reproductive and respiratory syndrome virus (PRRSV) is strongly affected by low-micromolar concentrations of cyclosporin A (CsA), an inhibitor of members of the cyclophilin (Cyp) family. In infected cells, the expression of a green fluorescent protein (GFP) reporter gene inserted into the PRRSV genome was inhibited with an IC_{50} of 5.2 µM, whereas the GFP expression of an EAV-GFP reporter virus was inhibited with an IC_{50} of 0.95 µM. Debio-064, a CsA analog that lacks its undesirable immunosuppressive properties, inhibited EAV replication with an IC_{50} that was three-fold lower than that of CsA, whereas PRRSV-GFP replication was inhibited with an IC_{50} similar to that of CsA. The addition of 4 µM CsA after infection prevented viral RNA and protein synthesis in EAV-infected cells, and CsA treatment resulted in a 2.5 to 4-log reduction of PRRSV or EAV infectious progeny. A complete block of EAV RNA synthesis was also observed in an *in vitro* assay using isolated viral replication structures. The siRNA-mediated knockdown of Cyp family members revealed that EAV replication strongly depends on the expression of CypA, but not CypB. Furthermore, upon fractionation of intracellular membranes in density gradients, CypA was found to cosediment with membranous EAV replication structures, which could be prevented by CsA treatment. This suggests that CypA is an essential component of the viral RNA-synthesizing machinery.

INTRODUCTION

The replication of RNA viruses strongly depends on their successful interplay with the host cell at multiple levels. By now, a wide variety of host cell proteins have been implicated in RNA virus replication and some of these might in fact constitute interesting targets for antiviral therapy [60]. Thus, the possibility to target host factors rather than viral proteins is receiving increasing attention as an alternative and promising antiviral approach (reviewed in [130, 131]). In contrast to antiviral therapy that aims to inhibit viral protein functions, the use of drugs targeting host factors should not lead to drug resistance, which is a common problem when combating RNA viruses due to their high mutation rate and potential for rapid adaptation.

The drug cyclosporin A (CsA) was previously found to inhibit the replication of a number of RNA viruses [271-275]. Recently, multiple laboratories, including our own, reported that also the replication of various (human) coronaviruses, including SARS-coronavirus (SARS-CoV), can be inhibited by CsA treatment [276-278]. This drug affects the function of several members of the cellular cyclophilin (Cyp) protein family, which consists of peptidyl-prolyl isomerases (PPIase) that act as chaperones to facilitate protein folding, and are involved in protein trafficking and immune cell activation [279, 280]. Although Cyps share many similarities in terms of structure and activity, important differences in specific functions and subcellular localization have been documented [280]. In line with the inhibition of virus replication by CsA, Cyp family members were identified as essential host factors in the replicative cycle of several virus groups (reviewed in [281]).

The drug CsA has been widely used as an immunosuppressant, e.g. in organ transplant patients [282], as its binding to various Cyps impairs calcineurin activity and abrogates the T cell response. As Cyps appeared to be relevant targets for antiviral therapy, several Cyp inhibitors have been developed that lack the immunosuppressive properties of CsA, which would be an undesirable side-effect during antiviral therapy. The efficacy of several of such compounds, e.g. Debio-025 and NIM811, is currently being explored in clinical trials for the treatment of hepatitis C virus (HCV) infection [283-285].

Since the replication of coronaviruses like SARS-CoV is inhibited by CsA [276, 277], we investigated whether this drug also inhibits the distantly related arteriviruses, which together with the coronavirus and ronivirus families constitute the order Nidovirales [286]. The arterivirus porcine reproductive and respiratory syndrome virus (PRRSV) is one of the leading veterinary pathogens, causing an estimated annual loss of 664 million dollars in the swine industry in the USA alone [27]. Equine arteritis virus (EAV), in addition to being a relevant horse pathogen, has been used for decades as a model to dissect the molecular details of arterivirus and nidovirus replication [287].

Arteriviruses are positive-stranded RNA viruses with a genome size of about 13-16 kb [37]. Their complex genome expression strategy involves genome translation to

produce the polyprotein precursors for the viral nonstructural proteins (nsps) as well as the synthesis of a nested set of subgenomic (sg) mRNAs to express the structural proteins [40]. The viral nsps, presumably together with various host factors, are thought to assemble into membrane-associated replication and transcription complexes (RTCs) that drive viral RNA synthesis (for recent reviews, see [37, 47]). Arterivirus RNA synthesis was reported to be associated with a virus-induced network of endoplasmic reticulum (ER)-derived membrane structures, including large numbers of double-membrane vesicles [29]. Many arteriviral proteins were found to be associated with these membrane structures, on which viral RNA synthesis was found to depend [33, 52]. However, thus far, the identity and role of proviral host factors involved in the replicative cycle of arteriviruses has remained largely unexplored.

Using EAV and PRRSV, our studies on the inhibition of nidovirus replication by CsA have now been extended to arteriviruses and explored the mechanism of action of the compound in more detail. We show that low micromolar concentrations of CsA can fully block arterivirus RNA synthesis and that the non-immunosuppressive cyclophilin inhibitor Debio-064 is an even more potent inhibitor. These compounds probably exert their effect through their inhibition of CypA, as RNAi-mediated knockdown of CypA strongly affected EAV RNA synthesis and CypA was found to cosediment with EAV replication structures.

MATERIALS AND METHODS

Cell culture, infection, and virus titration

BHK-21 [288], Vero E6 [220], and MARC-145 cells [289] were cultured as described previously. 293/ACE2 cells [74] were cultured in Dulbecco's modified Eagle's medium (DMEM; Lonza) supplemented with 8% FCS, 100 U/ml of penicillin and 100 µg/ml of streptomycin, 2 mM L-Glutamine, and 12 µg/ml Blasticidin (PAA). A cell culture-adapted derivative of the EAV Bucyrus isolate [290] and GFP-expressing recombinant EAV [291] were used to infect monolayers of BHK-21, Vero E6, and 293/ACE2 cells at an MOI of 5 as described previously [220, 288]. MARC-145 cells were infected with a GFP-expressing recombinant PRRSV (SD01-08-GFP) at an MOI of 0.1 as previously described [292]. EAV titers in cell culture supernatants were determined by plaque assay on BHK-21 cells [288], whereas PRRSV titers were determined by fluorescent focus assay (FFA) on MARC-145 cells, as described previously [293]. For IC_{50} determinations, cells were grown in black 96-well plates (Greiner), infected with EAV-GFP or PRRSV-GFP and treated with compounds in octuplet. GFP reporter expression was quantified by measuring fluorescence in a 96-well plate reader, using an excitation wavelength of 485 nm and emission wavelength of 535 nm.

Antibodies and drugs

Rabbit polyclonal antibodies against CypA (Abcam), CypB (Abcam), and Calnexin (BD), a goat polyclonal antiserum against GAPDH (Santa Cruz), and a mouse monoclonal antibody (mAb) against β-actin (Sigma) were used. Rabbit antisera recognizing the EAV replicase subunits nsp3 [201] and nsp9 [52], and the EAV membrane (M) protein [220], and a mAb against the EAV nucleocapsid (N) protein [294] have been described previously. The cyclophilin inhibitors CsA (Sigma) and Debio-064 (Debiopharm, Switzerland) were dissolved in DMSO. CsA was stored as 50 mg/ml stock at -20°C and Debio-064 was stored as a 10 mM stock at 4°C in aliquots for single use. The IC_{50} of inhibitors was calculated with Graphpad Prism 5 using the nonlinear regression model.

Immunofluorescence microscopy

EAV-infected or mock-infected BHK-21 cells, grown on coverslips at 39.5°C, were fixed with 3% paraformaldehyde in PBS, permeabilized with 0.1% Triton X-100, and processed for immunofluorescence microscopy as described previously [33]. Specimens were examined with a Zeiss Axioskop 2 fluorescence microscope with an Axiocam HRc camera and Zeiss Axiovision 4.4 software.

Western blot analysis

After SDS-PAGE, proteins were transferred to Hybond-LFP membranes (GE Healthcare) by semi-dry blotting. Membranes were blocked with 1% casein in PBS containing 0.1% Tween-20 (PBST), and were incubated with anti-nsp3 (1:2000), anti-nsp9 (1:2000), anti-M (1:2000), anti-N (1:10,000), anti-CypA (1:1000), anti-CypB (1:2000), or anti-β-actin (1:50,000) antisera, diluted in PBST with 0.5% casein. Biotin-conjugated swine-anti-rabbit IgG (1:2000) or goat-anti-mouse IgG (1:1000) antibodies (DAKO) and Cy3-conjugated mouse-anti-biotin (1:2500) were used for detection. Blots were scanned with a Typhoon 9410 imager (GE Healthcare) and analyzed with ImageQuant TL software.

Isolation of EAV RTC-containing replication structures and *in vitro* RNA synthesis assays

EAV replication structures were isolated from BHK-21 or Vero E6 cells, and *in vitro* RNA synthesis assays were performed essentially as described previously [52]. In short, approximately 1×10^8 EAV-infected BHK-21 or Vero E6 cells were harvested at 6 or 7 h p.i., and cells were lysed to obtain a post nuclear supernatant (PNS) [52]. A standard *in vitro* RNA synthesis assay contained 20 μl of PNS (the equivalent of 6×10^4 cells) from EAV-infected BHK-21 cells, 5 μl of an inhibitor solution or 5 μl of RTC dilution buffer (control). Following gel electrophoresis, ^{32}P-labeled reaction products were analyzed by denaturing agarose gel electrophoresis and by exposing a PhosphorImager screen directly

to the dried gel, after which screens were scanned with a Typhoon 9410 imager (GE Healthcare), and incorporation of label was quantified using ImageQuant TL software.

Density gradient fractionation

Subcellular fractionation of PNS was performed in continuous 0-30% OptiPrep density gradients in RTC dilution buffer. The gradients were prepared in 13.2 ml Ultra Clear centrifugation tubes (Beckman Coulter) using a Gradient Master (Biocomp). One ml of PNS from Vero E6 cells was carefully loaded on top of the preformed gradient. After centrifu-
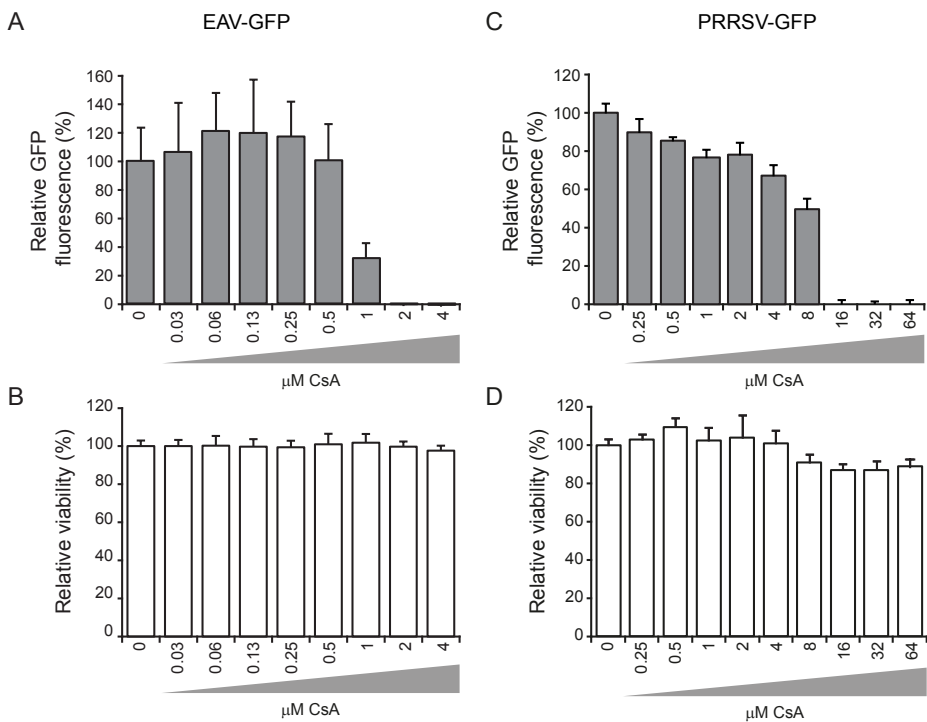

Fig. 1. Cyclosporin A treatment blocks EAV-GFP and PRRSV-GFP replication. (A) BHK-21 cells were infected with EAV-GFP at a MOI of 5 and at 1 h p.i. the inoculum was replaced by medium containing different concentrations of CsA, as indicated on the x-axis. Cells were fixed at 18 h p.i. and GFP reporter expression was quantified and normalized to the GFP signal of control cells (100%) treated with DMSO (solvent concentration equal to that of the cultures that received 4 µM CsA). (B) The effect of CsA on cell viability, compared to untreated control cells (100%), was determined using the CellTiter 96® AQ$_{ueous}$ Non-Radioactive Cell Proliferation Assay (Promega). Graphs show the results (avg and SD) of a representative experiment in quadruplo. (C) MARC-145 cells were infected with PRRSV-GFP at a MOI of 0.1 and at 1 h p.i. the inoculum was replaced by medium with CsA. Cells were fixed at 24 h p.i. and GFP reporter expression was quantified and normalized to the signal in solvent-treated control cells (100%). (D) The effect of CsA on the viability of the MARC-145 cells, compared to untreated control cells (100%). Graphs show the results (avg and SD) of a representative experiment (n=8). All experiments were repeated at least twice.

gation for 17 h at 48,000 x g in a SW41 rotor at 4°C, the gradient was fractionated into 0.5 ml fractions. The density of each fraction was determined with a refractometer (GETI).

Metabolic labeling of viral RNA synthesis

Labeling of viral RNA with [³H]uridine was performed essentially as described previously [295]. Briefly, at 4.5 h p.i. 4×10^5 EAV-infected BHK-21 cells in 4-cm² dishes were given medium containing 10 µg/ml actinomycin D (ActD; Sigma-Aldrich), and either 4 µM CsA or 0.01% DMSO as solvent control. After 1 h, viral RNA synthesis was labeled by adding 100 µCi of [³H]uridine to the medium. The ³H-labeled RNAs were isolated, separated in denaturing agarose gels, and visualized by fluorography. To verify that equal amounts of total RNA were loaded, the gel was hybridized with a ³²P-labeled oligonucleotide probe (5'- TTCACGCCCTCTTGAACTCTCTCTTC -3') recognizing 28S ribosomal RNA, as described previously [52].

RNA interference

ON-TARGETplus smartpool siRNA duplexes (Dharmacon) against CypA (PPIA; cat. nr. L-004979-04) and CypB (PPIB; cat. nr. L-004606-00) were used to silence CypA and CypB expression in 293/ACE2 cells. A non-targeting siRNA (D-001810-10) was used as a control and a GAPDH-targeting siRNA (D-001830-10) was used to monitor transfection and knockdown efficiency. Stock solutions of 2 µM were prepared by dissolving siRNAs in 1x siRNA buffer (Dharmacon). For transfection of cells in 96-well clusters, 1×10^4 293/ACE2 cells per well were transfected with a 100-µl mixture containing 100 nM siRNA, 0.2 µg DharmaFECT1 (Dharmacon), OptiMEM (Invitrogen), and antibiotic-free culture medium, according to the manufacturer's instructions. For cells in 12-well clusters, 600 µl transfection mixtures were used. Medium was replaced at 24 h post transfection (p.t.) by antibiotic-free culture medium, and at 48 h p.t. cells were infected with EAV-GFP or wt EAV. Duplicate cultures were used to either prepare lysates to analyze protein expression levels or to monitor cell viability using the CellTiter 96® AQ$_{ueous}$ Non-Radioactive Cell Proliferation Assay (Promega), according to the manufacturer's instructions.

RESULTS

EAV-GFP and PRRSV-GFP replication is inhibited by CsA.

The effect of CsA on arterivirus replication was investigated in cell culture using two representatives of the arterivirus family, EAV and PRRSV (European genotype). For the initial experiments, we employed GFP-expressing recombinant viruses, since quantification of GFP expression provides a rapid and reliable method to detect inhibition of virus replication. BHK-21 cells were grown in 96-well plates and infected at an MOI of

5 with GFP-expressing recombinant EAV [291]. Upon removal of the inoculum (1 h p.i.), medium containing 0.03 to 4 μM of CsA was given, and at 18 h p.i. cells were fixed and GFP expression was quantified. We observed a strong dose-dependent inhibition of EAV-GFP replication (Fig. 1A) in the absence of significant cytotoxic effects at the CsA concentrations used (Fig. 1B). The half maximal inhibitory concentration (IC_{50}) of CsA for EAV-GFP replication in BHK-21 cells was determined to be 0.95 μM.

A similar experiment was performed with PRRSV-GFP in MARC-145 cells (Fig. 1C). Although less sensitive to CsA treatment than EAV-GFP, the replication of PRRSV-GFP was completely blocked at 16 μM of CsA and an IC_{50} of 5.22 μM was determined. Cell viability was only slightly affected by CsA concentrations above 4 μM (Fig. 1D).
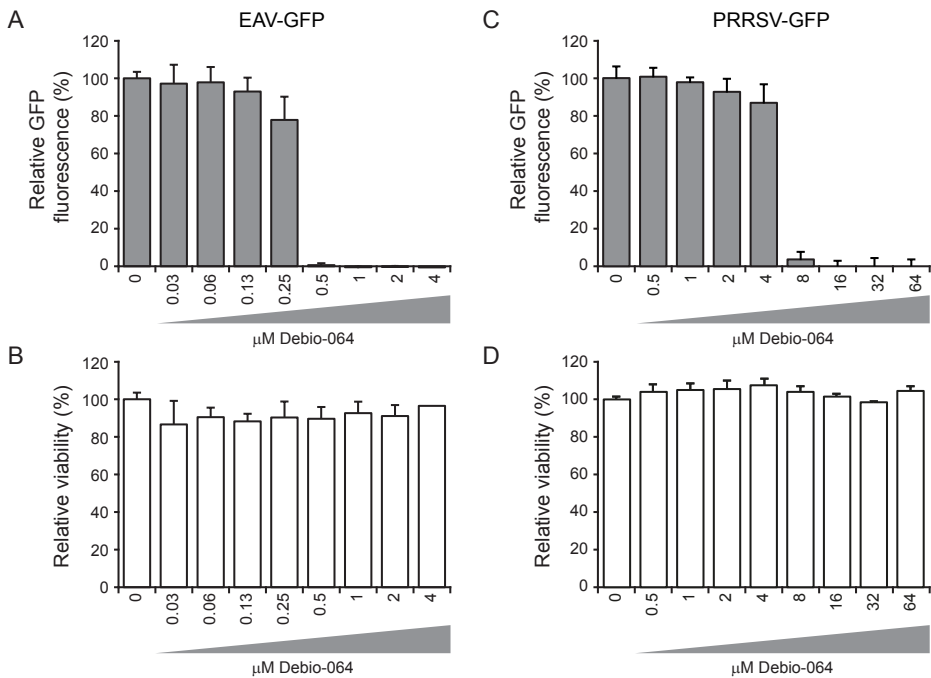

Fig. 2. The CsA analog Debio-064 blocks EAV-GFP and PRRSV-GFP replication. (A) EAV-GFP-infected BHK-21 cells (MOI of 5) were incubated with various concentrations of Debio-064 from 1 h p.i. onwards. Cells were fixed at 18 h p.i. and GFP reporter expression was quantified and normalized to the GFP signal of control cells (100%) that were treated with DMSO (solvent concentration equal to medium containing 4 μM Debio-064). (B) The effect of Debio-064 on BHK-21 cell viability, compared to untreated control cells (100%). (C) PRRSV-GFP-infected MARC-145 cells (MOI of 0.1) were incubated with various concentrations of Debio-064 from 1 h p.i. onwards. Cells were fixed at 24 h p.i. and GFP reporter expression was quantified and normalized to the GFP signal of control cells (100%) that were treated with DMSO. (D) The effect of Debio-064 on MARC-145 cell viability, compared to control cells (100%). Results (avg and SD) of a representative quadruplicate experiment are shown and all experiments were repeated at least twice.

The cyclophilin inhibitor Debio-064 blocks EAV-GFP and PRRSV-GFP replication.

Although CsA has been found to effectively block the replication of various RNA viruses in cell culture [281], its use in antiviral therapy would be complicated by the immune suppression [296] that is a major side effect. Therefore, several alternative Cyp inhibitors have been developed that lack the immune suppressive properties of CsA, like SCY-635, NIM811, and Debio-025, which all block HCV replication [284, 285, 297].

In this study we tested whether the non-immunosuppressive Cyp inhibitor Debio-064 is able to block EAV-GFP and PRRSV-GFP replication (Fig. 2A). Debio-064 is a structurally modified cyclosporin exhibiting an approximately 5-fold higher affinity for CypA in comparison to CsA. Debio-064 is 300-fold less active than CsA at inhibiting mouse T-cell proliferation induced by concanavalin A, suggesting that the compound does not inhibit calcineurin [298]. EAV-GFP-infected BHK-21 cells (Fig. 2B) or PRRSV-GFP-infected MARC-145 cells (Fig. 2D) were treated with various non-cytotoxic concentrations of Debio-064 and viral replication was quantified as described for CsA treatment. Compared to CsA, Debio-064 had a stronger inhibitory effect on EAV-GFP replication. At a concentration of 0.5 µM Debio-064, the EAV-GFP signal was hardly detectable (Fig. 2A), and an IC_{50} of 0.29 µM was determined, which is about 3-fold lower than that of CsA. For PRRSV-GFP, an almost complete block in GFP expression was observed at 8 µM and an IC_{50} of 5.14 µM was determined (Fig. 2C), which is comparable to the inhibitory effect of CsA on PRRSV-GFP replication.

CsA and Debio-064 prevent arterivirus protein expression.

In our initial experiments, we tested the effect of CsA on the replication of a GFP-expressing recombinant EAV. To verify that also wild-type (wt) EAV replication could be inhibited by the drug, we analyzed wt EAV-infected BHK-21 cells that were treated with 0.25 to 8 µM of CsA. At 6 h p.i., cells were lysed and lysates were subjected to Western blot analysis. The expression of viral nonstructural proteins (the nsp5-8 precursor and nsp9) and the structural M and N proteins was hardly detectable after 4-µM CsA treatment, while a clear reduction in protein expression could already be observed at 2 µM of CsA (Fig. 3A). As observed for EAV-GFP, Debio-064 had a stronger inhibitory effect than CsA on the replication of wt EAV. Viral protein expression was clearly reduced in the presence of 0.5 µM of the drug, and became almost undetectable at 1 µM of Debio-064 (Fig. 3B).

The effect of CsA and Debio-064 was further characterized by immunofluorescence microscopy of infected cells. For wt EAV, dsRNA (data not shown) and viral proteins were undetectable after a dose of 4 µM CsA (Fig. 3C) or 1 µM Debio-064 (Fig. 3D). In the case of PRRSV-GFP-infected MARC-145 cells (data not shown) maximal inhibition was observed at a 16 µM CsA dose. However, as previously observed for coronavirus-infected Vero E6, 17Cl1, or Huh7 cells [276], a small fraction of the MARC-145 cells remained capable of
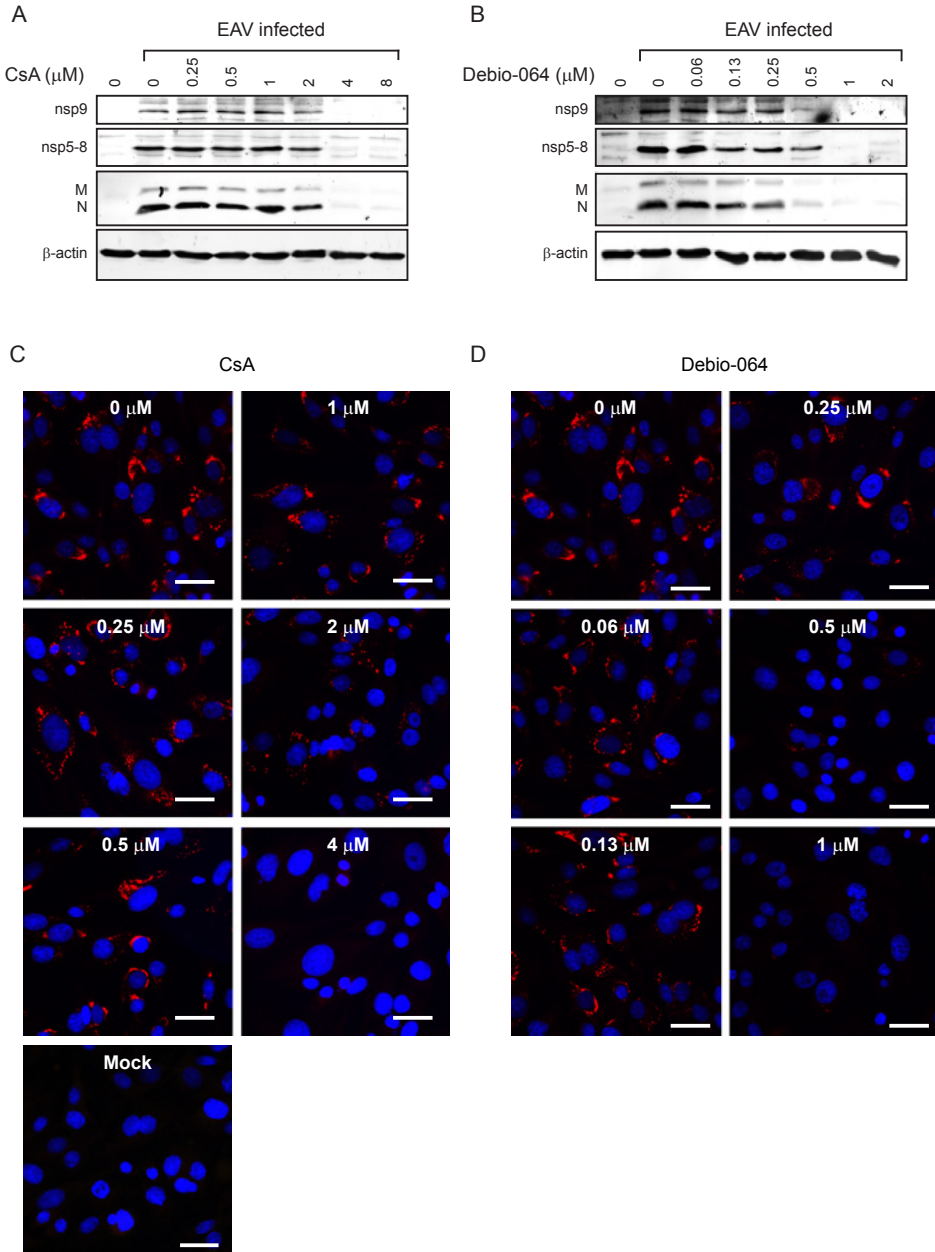
A

EAV infected

CsA (μM)   0   0   0.25   0.5   1   2   4   8

nsp9

nsp5-8

M
N

β-actin

B

EAV infected

Debio-064 (μM)   0   0   0.06   0.13   0.25   0.5   1   2

nsp9

nsp5-8

M
N

β-actin

C

CsA

0 μM	1 μM
0.25 μM	2 μM
0.5 μM	4 μM
Mock	

D

Debio-064

0 μM	0.25 μM
0.06 μM	0.5 μM
0.13 μM	1 μM

Fig. 3. CsA and Debio-064 treatment block viral protein expression in cells infected with wild-type EAV. BHK-21 cells were infected with EAV (MOI 5) and treated from 1 h p.i. on with CsA (A) or Debio-064 (B) at the concentration indicated above each lane. Cells were lysed at 6 h p.i. and viral protein expression was analyzed by SDS-PAGE and Western blotting with antibodies against nsp9 and nsp5-8, the M protein and the N protein. β-actin was used as loading control. For immunofluorescence microscopy, mock-infected or EAV-infected and CsA- (C) or Debio-064-treated (D) cells were fixed at 6 h p.i. and stained with an anti-nsp3 antiserum. The drug concentrations used are indicated in each panel. Scale bar, 50 μm.

supporting PRRSV-GFP virus replication, even at high CsA doses of up to 64 µM (data not shown). We did not observe such a small, residual population of apparently drug-insensitive cells in EAV-infected BHK-21 cultures treated with either CsA or Debio-064 (Fig. 3C-D).

CsA and Debio-064 block the production of arterivirus infectious progeny.

To assess to which extent CsA and Debio-064 treatment affected infectious progeny titers, we performed plaque assays to measure EAV titers at 12 h p.i. using supernatants from infected (MOI 5) BHK-21 cells that had been treated with CsA or Debio-064 (Fig. 4A). CsA strongly reduced EAV progeny titers, with an almost 4-log reduction at 4 µM CsA. Treatment probably completely abolished virus production as the titers observed after treatment with 4 µM CsA were similar to those measured at 1 h p.i., which likely reflected the remainder of the high MOI inoculum used (data not shown). These data correlated well with the barely detectable expression of nsp5-8, nsp9, M, and N protein and the lack of dsRNA after treatment with 4 µM CsA (Fig. 3A and C). Treatment with Debio-064 also resulted in a ~4-log reduction of infectious progeny at 2 µM, while a 2- to 3-log reduction was already achieved by treatment with 1 µM of the compound.

Using a fluorescent focus assay, we also analyzed the production of PRRSV-GFP infectious progeny in 24 h p.i.-culture supernatants of CsA-treated MARC-145 cells. As observed for EAV, the production of PRRSV-GFP infectious progeny was affected by CsA treatment, although significantly higher concentrations were required. At 16 µM of CsA, a ~1.5-log reduction in the yield of infectious progeny was observed, while an apparently complete block (2.5-log reduction) required a dose of 32 µM (Fig. 4B; grey
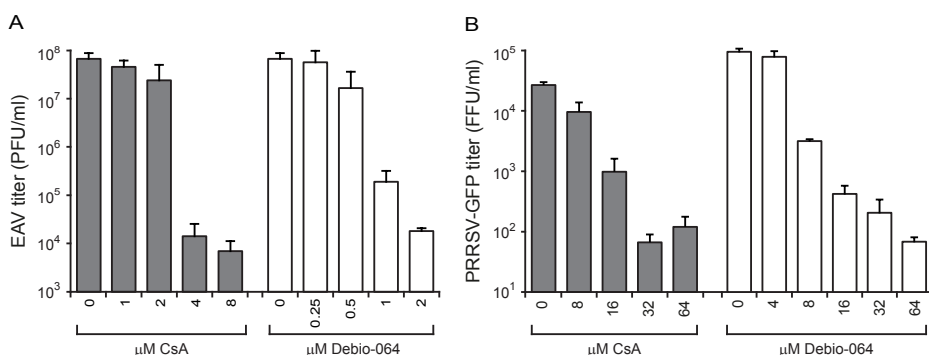

Fig. 4. Treatment of infected cells with cyclophilin inhibitors strongly reduces arterivirus yields. (A) EAV-infected BHK-21 cells (MOI of 5) were treated with various concentrations of CsA (grey bars) or Debio-064 (white bars) from 1 h p.i. onwards, and virus titers in the culture medium at 12 h p.i were determined by plaque assay. (B) MARC-145 cells infected with PRRSV-GFP (MOI 0.1) were treated from 1 h p.i. onwards with the CsA (grey bars) or Debio-064 (white bars) concentrations indicated below the x-axis and virus titers in the medium at 24 h p.i. were determined by fluorescent focus assay.

bars). Treatment with Debio-064 resulted in a ~1.5-log reduction at 16 μM and a ~2.5-log reduction of infectious progeny at 32 μM (Fig. 4B; white bars), which is comparable to the reduction in PRRSV progeny observed upon CsA treatment.

Cyclophilin inhibitors affect EAV RNA synthesis both *in vivo* and *in vitro*.

The above experiments showed that CsA can effectively block both EAV and PRRSV replication in cell culture. To establish that this lack of viral protein synthesis was due to a block of viral RNA synthesis, we measured the effect of CsA treatment on EAV RNA
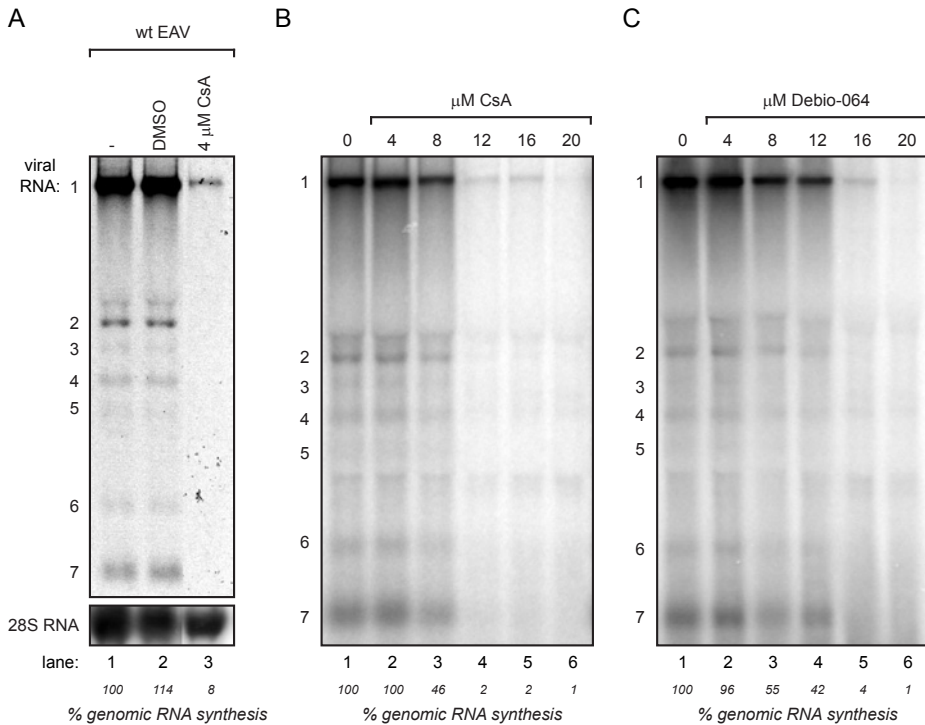

Fig. 5. The *in vitro* and *in vivo* RNA-synthesizing activity of EAV RTCs can be blocked by CsA or Debio-064 treatment. (A) Metabolic labeling of EAV-infected cells with [³H]uridine between 5.5 and 6.5 h p.i. in the presence or absence of 4 μM CsA. Total RNA was isolated, analyzed in denaturing agarose gels, and detected by fluorography. The amount of [³H]uridine that was incorporated into viral genomic RNA was quantified and normalized to that in EAV-infected,untreated control cells (100%). 28S RNA detected by hybridization with a ³²P-labeled probe (lower panel) was used as a control to correct for variations in loading during viral RNA quantification. (B and C) Semi-purified RTCs isolated from EAV-infected BHK-21 cells at 6 h p.i. were used in an *in vitro* RNA synthesis assay in which [³²P]CTP is incorporated into viral RNA. Reactions, performed in the presence of various concentrations of CsA (B) or Debio-064 (C) as indicated above the lanes, were terminated after 100 minutes. RNA was isolated and reaction products were analyzed in denaturing formaldehyde agarose gels. The positions of the genomic RNA (1) and sub-genomic RNAs (2-7) are indicated next to the gels.

synthesis in infected Vero E6 cells *in vivo*, by metabolic labeling with [^{3}H]uridine (in the presence of actinomycin D). When 4 μM of CsA was given at 4.5 h p.i., ^{3}H incorporation into viral RNA during a pulse labeling from 5.5 to 6.5 h p.i. was reduced to 8% of the incorporation measured for non-treated control cells (Fig. 5A). To obtain more insight into the mechanism by which CsA inhibits arterivirus replication, we tested its effect in a previously developed *in vitro* assay to study the RNA-synthesizing activity of semi-purified EAV RTCs [52]. These assays were performed with PNS from EAV-infected BHK-21 cells and the reactions, during which ^{32}P-labeled CTP is incorporated into viral RNA, were conducted in the presence of various concentrations of CsA. In the absence of the drug, *in vitro* synthesis of EAV genomic and sg RNAs was observed (Fig. 5B, lane 1), as documented previously [52]. RNA synthesizing activity was completely abolished when the reaction was performed in the presence of 12 μM of CsA (lane 4), while a >50% reduction of viral RNA synthesis was observed in the presence of 8 μM CsA (lane 3). Comparable results were obtained with Debio-064, which also caused a >50% reduction of EAV RTC activity around 8 μM and a complete inhibition at 16 μM Debio-064 (Fig. 5C; lane 3 and 5). These data strongly suggest that Cyp inhibitors can directly affect the RNA-synthesizing capacity of the membrane-associated EAV RTCs in PNS samples. We recognize that the concentrations needed to fully block EAV RTC activity *in vitro* are ~3-fold higher than those required to block virus replication in cell culture. This might be due to differences in the experimental set-up, as the PNS used for the *in vitro* reaction constituted a concentrated preparation of RTCs (and host factors), and reaction conditions might influence the interaction between Cyps and their inhibitor.

EAV replication depends on cyclophilin A.

CsA is known to inhibit the PPIase activity of several members of the cyclophilin family. In particular CypA and CypB have been implicated in the replication of several viruses (reviewed in [281]). We therefore analyzed the effect of siRNA-mediated knock-down of CypA and CypB expression levels on the replication of EAV-GFP. We made use of the same human 293/ACE2 cells that we previously used to study the role of Cyps in SARS-CoV replication [276]. This cell line was also susceptible to EAV infection, although only ~40% of the cells became GFP-positive after a high MOI infection with EAV-GFP, as judged by immunofluorescence microscopy of infected cells fixed at 8 h p.i. (data not shown).

Knockdown of CypA and CypB expression was monitored by Western blot analysis and a ~80% reduction of expression was typically observed compared to the level in control cells transfected with a non-targeting control siRNA (Fig. 6A). Depletion of CypA or CypB did not have a significant effect on cell viability during the 48 h of the knockdown experiment (Fig. 6B). Compared to control cells, knockdown of CypB expression did not influence GFP reporter expression when these cells were infected with EAV-GFP, in which GFP fluorescence was measured at 24 h p.i. (Fig. 6C). In contrast, knockdown
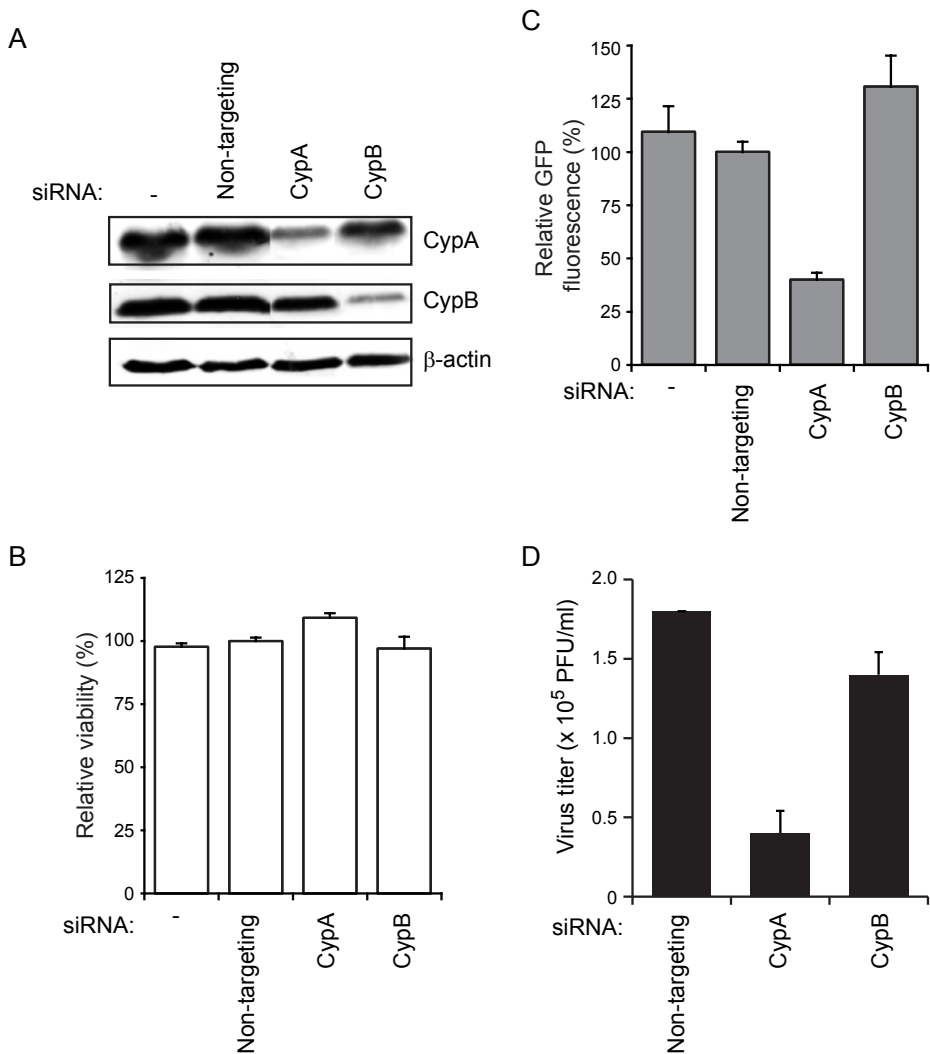
Fig. 6. RNAi-mediated knock-down of CypA, but not CypB, strongly affects EAV replication. 293/ACE2 cells were transfected with a non-targeting control siRNA or siRNAs targeting CypA or CypB. Knockdown of CypA (A, upper panel) and CypB (A, middle panel) levels was monitored by Western blotting with CypA- and CypB-specific antisera. β-actin was used as loading control. (B) Viability of cells 48 h post transfection with the various siRNAs normalized to the MTS signal of cells transfected with the non-targeting control siRNA (100%). (C) GFP reporter expression of cells transfected with the siRNAs indicated below the graph, and infected 48 h post-transfection with EAV-GFP at an MOI of 5. Cells were fixed at 24 h p.i. and GFP fluorescence was quantified and normalized to that in infected cells transfected with non-targeting siRNA. (D) Virus titers at 32 h p.i. in the culture medium of cells transfected with the siRNAs indicated below the graph, and infected 48 h post transfection with wt EAV at an MOI of 0.01.

of CypA resulted in a ~60% reduction of the GFP signal in EAV-GFP-infected cells, compared to that of the control cells (Fig. 6C). Furthermore, wt EAV titers at 32 h p.i. in the culture medium of infected 293/ACE2 cells (MOI 0.01) that had been depleted for CypA showed a ~4-fold decrease in virus progeny compared to control cells (Fig 6D). These data strongly suggest that EAV replication and the production of virus progeny depend on the availability of the host factor CypA.

Cyclophilin A cosediments with EAV RTCs.

Since our RNAi experiments suggested that EAV RNA synthesis depends on the availability of CypA, we investigated whether CypA cosediments with EAV RTC-containing membranes. We therefore fractionated post-nuclear supernatants (PNS) from EAV-infected and mock-infected Vero E6 cells in a 0-30% OptiPrep density gradient. Gradient fractions were analyzed by Western blot using antisera against CypA, CypB, several EAV nsps, and various organelle marker proteins (Fig. 7). Densities in the gradient ranged from 1.04 g/ml to 1.18 g/ml (Fig. 7A) and the low-density fractions of both EAV-infected and mock-infected PNS contained the cytosolic marker glyceraldehyde 3-phosphate dehydrogenase (GAPDH), while several organelle markers, like the ER protein calnexin and the mitochondrial marker CoxIV (data not shown) were found in higher-density fractions (Fig. 7B-C). This confirmed the separation of membrane-containing fractions from the cytosol. The membrane-associated EAV RTCs, detected with an antiserum directed against nsp9 (RdRp), sedimented at densities around 1.15 g/ml (Fig. 7C). The nsp9-containing fraction also contained significant amounts of the normally cytosolic CypA (Fig. 7C). Upon density gradient fractionation of PNS from uninfected cells CypA was only found in the low-density cytosolic fractions (Fig. 7B), but in PNS from EAV-infected cells a fraction of CypA was found to cosediment with the RTC-containing membranes (compare fraction 3 in Fig. 7B and C). CypB, being an ER-associated protein, was observed in the high-density gradient fractions of both mock- and EAV-infected cell lysates (Fig. 7B). Therefore the protein was present in the fractions containing the EAV RTCs, in particular in the nsp9-containing fraction (Fig. 7C, fraction 3-4), but was clearly more dispersed in the gradient with mock-infected PNS.

To analyze whether CsA can prevent the cosedimentation of CypA with EAV RTCs, we pretreated the PNS from EAV-infected cells with 12 µM of CsA - the concentration that completely inhibited EAV RTC activity *in vitro* - for 30 minutes on ice before separating the material in an OptiPrep density gradient. Subsequently, the high-density nsp9-containing membrane fractions were analyzed for the presence of CypA by Western blotting (Fig. 7D). In the absence of CsA a clear cosedimentation of CypA and nsp9 was observed, while CypA was no longer detectable in the high-density nsp9-containing fraction of CsA-treated lysates. This suggests that CsA can prevent the cosedimentation of CypA with the membrane-associated EAV RTCs.
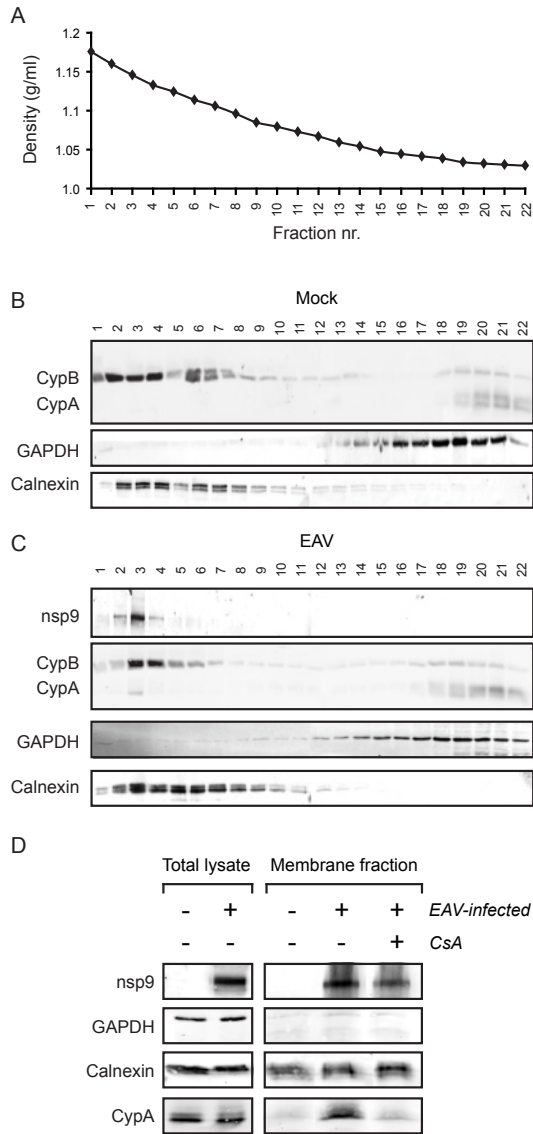
Fig. 7. Co-sedimentation of CypA with EAV RTCs in density gradients. The post-nuclear supernatant of EAV- and mock-infected Vero E6 cells was fractionated using a continuous 0-30% OptiPrep density gradient. (A) Densities of the fractions were determined with a refractometer. (B) Distribution of CypA, CypB, the cytosolic marker protein GAPDH, and ER marker protein calnexin in density gradient fractions of mock-infected cell lysates as analyzed by Western blotting. (C) Distribution of CypA, CypB, the cytosolic marker protein GAPDH, ER marker protein calnexin and EAV RdRp nsp9 in density gradient fractions of EAV-infected cells as analyzed by Western blotting. (D) Before loading on a 0-30% OptiPrep gradient, PNS was pretreated with 12 μM CsA for 30 minutes on ice. Western blot analysis of the sedimentation of CypA, the ER marker protein Calnexin, and the cytosolic marker protein GAPDH in nsp9-containing membrane fractions of CsA-treated and untreated PNS, and a fraction with the same density prepared from mock-infected cells.

DISCUSSION

Our study shows that arterivirus replication can be inhibited by the cyclophilin inhibitor CsA and the non-immunosuppressive CsA-analog Debio-064, which inhibit EAV RNA synthesis, likely through their effect on the host protein CypA that appears to be recruited to EAV RTCs. CsA inhibits the PPIase function of CsA-sensitive Cyp family members, like CypA, by binding to their active site [279]. We here show that low-micromolar concentrations of CsA can block the replication of both EAV and PRRSV, two prominent representatives of the arterivirus family. PRRSV-GFP replication was inhibited with an IC_{50} of 5.22 µM and an almost complete block was observed upon treatment with 16 µM CsA (Fig. 1C). These values are comparable to those previously observed for the inhibition of coronavirus replication by CsA [276, 277]. Compared to PRRSV and coronaviruses, the inhibitory effect of CsA was even stronger for EAV, for which we calculated IC_{50} values of 0.95 µM (Fig. 1A). The IC_{50} values obtained for arteriviruses are in the range of those observed for other viruses, like HCV [274, 299], several flaviviruses [275], vaccinia virus [300], and HIV-1 [272]. A remarkable and yet not understood phenomenon is that a small fraction (1-5%) of PRRSV-infected MARC-145 cells and, previously, coronavirus-infected Vero E6, 17Cl1, or Huh7 cells [276] appeared to be refractive to CsA treatment, even at high concentrations. This effect was not observed for EAV-infected BHK-21 cells (Fig. 3C), which might be explained by the higher sensitivity of EAV to the compound. In any case, the fact that the distantly related coronaviruses [276, 277] and arteriviruses can both be inhibited by CsA suggests the nidovirus-wide conservation of a cyclophilin-dependent function in viral replication.

Previously, CsA was found to inhibit the replication of a variety of RNA viruses, including important human pathogens like HCV, HIV-1, and Dengue virus (reviewed in [281]). For example, both CypA and CypB were found to specifically interact with the flaviviral nonstructural proteins NS5A and NS5B and these interactions are sensitive to CsA treatment [273, 301-303]. In the case of the interaction of CypA with HCV NS5A, the PPIase activity of the former was proposed to induce a conformational change in the latter [304] that promotes RNA binding to NS5A and enhances RNA replication [305]. Chatterji *et al*. reported that, in addition to the CypA-NS5A interaction, HCV replication also depends on the binding of CypA to the enzymatic pocket of NS5B, the viral RdRp, thus enhancing its affinity for RNA. On the other hand, PPIase-defective CypA failed to interact with HCV NS5B [306], suggesting that the isomerase activity of CypA is an essential factor in the interaction with NS5B that promotes HCV replication. Liu *et al*. showed that the binding of CypA to NS5B mediates the proper folding of enzymatically active NS5B and facilitates the incorporation of the latter into replication complexes. The interaction between CypA and NS5B can be inhibited by CsA [307]. In addition, Kaul *et al*. showed that the development of resistance against the Cyp inhibitor Debio-025

involved mutations (V2440A and V2440L) in HCV NS5B that are close to the NS5A/NS5B cleavage site. These are thought to delay processing of the NS5A/NS5B junction, thus extending the time during which the CypA binding site in NS5B is accessible [308]. As a result, lower amounts of CypA would suffice to mediate the proper folding of NS5B and its incorporation into replication complexes. Similar functions were attributed to CypB, since also the interaction between CypB and NS5B was found to be essential for RNA binding by NS5B and for HCV replication as a whole [309]. Furthermore, Japanese encephalitis virus replication depends on the binding of CypB to NS4A and on CypB isomerase activity [273]. For a number of RNA viruses, CypA was found to be incorporated into newly formed virions, although the functional relevance of this finding remains to be addressed in more detail [271, 310, 311]. CypA also interacts with the SARS-CoV N protein [312] suggesting that the protein could be incorporated into virions [312], although coronavirus N proteins have also been implicated in viral RNA synthesis [313, 314] and are associated with intracellular replication structures [32].

We here show that expression of CypA is required for efficient EAV replication, as siRNA-mediated knockdown of CypA drastically reduced EAV-GFP replication (Fig. 6), while targeting CypB or Cyp40 (Fig. 6 and data not shown) had no effect. The importance of - the normally cytosolic - CypA was further substantiated by its co-sedimentation with RTC-containing membrane structures in the high-density gradient fractions of EAV-infected cell lysates. In such gradients, the sedimentation of the ER marker protein calnexin was essentially similar when comparing infected and mock-infected PNS (Fig. 7B-C). Furthermore, CsA treatment was able to prevent the sedimentation of CypA to the part of the gradient that also contained the EAV RTCs, following their biochemical isolation from infected cells (Fig. 7D), and the *in vitro* RNA synthesizing activity of such replication structures was found to be inhibited by CsA and Debio-064 (Fig. 5B-C). The distribution of CypB appeared to be less dispersed in gradients containing infected cell lysates compared to mock-infected lysates, even though EAV-GFP replication was not affected by the siRNA-mediated knockdown of CypB levels (Fig. 6). This suggests that although the subcellular localization of CypB might be affected by the extensive EAV-driven modification of intracellular membranes [29], this does not have a measurable effect on virus replication. By using fluorescence microscopy, colocalization of CypA and viral RTCs could not be observed, presumably because the fraction of CypA that localizes to replication structures is too small (data not shown). Interestingly, we could previously not measure an effect on SARS-CoV replication when CypA or CypB expression was (largely) silenced [276] in the same 293/ACE2 used here for our EAV studies. The ~20% residual Cyp expression that remained after siRNA-mediated knockdown may have been sufficient to support normal SARS-CoV replication, whereas it appears insufficient to support the efficient replication of the apparently more sensitive EAV, in line with the higher sensitivity of this arterivirus to CsA treatment.

As reported for HCV [305-307], the association of CypA with the EAV replication structures suggests the existence of a functional – presumably PPIase activity-dependent - interaction that is essential for virus replication. This member of the cyclophilin protein family appears to directly promote the RNA-synthesizing activity of the EAV RTC (Fig. 5). Based on studies that analyzed binding sites for CypA using a set of 40 potential CypA-inhibiting peptides [315], we identified several potential CypA binding sites in EAV nsp10, the viral helicase protein. A functionally important interaction with such a key enzyme in arterivirus RNA synthesis could certainly explain that efficient EAV replication depends on the availability of sufficient CypA. Clearly, at this moment, we cannot exclude (direct or indirect) interactions with any of the other viral proteins, including – in analogy to HCV [306] - the viral RdRp subunit (nsp9). In line with the ideas regarding the influence of CypA on the RNA-binding capacity of HCV NS5A and NS5B, EAV RTC-associated CypA may be involved in the proper folding or activation of viral enzymes and/or their binding to viral RNA, which might directly affect their function in RNA synthesis.

CsA analogs like Debio-025, NIM811, and SCY635, which have an increased affinity for Cyps and lack the undesired immunosuppressive effect of CsA [284, 285, 297], can be considered promising antiviral compounds, as they could block HCV replication almost completely and resistance to these compounds does not easily develop, compared to inhibitors directly targeting viral enzymes [316]. In our study we compared the inhibition of EAV and PRRSV replication by CsA with that caused by the non-immunosuppressive CsA-analog Debio-064. For Debio-064 we obtained an IC_{50} value of 0.32 µM, 3-fold lower than that of CsA (Fig. 2), which is in line with Debio-064's higher affinity for Cyps. We also observed an inhibitory effect of Debio-064 on PRRSV-GFP replication, although in contrast to EAV, its IC_{50} was similar to that of CsA. Therefore, more potent (non-immunosuppressive) CsA analogs not only constitute a promising class of molecules for the treatment of viral infections, but these compounds are also valuable research tools for mechanistic studies into the role of cyclophilins in the replication of nidoviruses and other +RNA viruses.

CHAPTER 3

ACKNOWLEDGMENTS